Research Article

Preparation of spray-coated surfaces from green-formulated superhydrophobic coatings

Eugene B. Caldona[1,2] · Jerry W. Sibaen[1] · Crissalyn B. Tactay[1] · Sierra Leone D. Mendiola[1] · Clyde B. Abance[1] · Marice P. Añes[1] · Faith Daser D. Serrano[1] · Marnoel Matthew S. De Guzman[1]

Received: 13 April 2019 / Accepted: 17 October 2019 / Published online: 22 November 2019

Abstract

This study involves the fabrication of green-based superhydrophobic coatings, which can be applied to a surface via a simple spraying technique. The coating formulation is green as it utilizes silica extracted from rice husks (RHA) and silver particles reduced and capped by cabbage (CRS), both of which are readily available and environmentally-benign. 12.5 wt% loading of the RHA in the coating was found to yield the best superhydrophobic behavior via contact angle measurement. By further introducing CRS, which induces repulsive forces preventing particle agglomeration, the resulting RHA/CRS-coated surfaces exhibited better anti-wetting behavior and improved stability and durability. In addition, the coating was also shown to possess self-cleaning property, pH resistance, and insensitivity to any touches. All of these reveal the potential of the green-formulated RHA/CRS coating as a cheaper and friendlier alternative in the quest for superhydrophobicity.

This work is dedicated to all hardworking and persistent Filipino researchers.

Electronic supplementary material The online version of this article (https://doi.org/10.1007/s42452-019-1510-4) contains supplementary material, which is available to authorized users.

✉ Eugene B. Caldona, ebcaldona@slu.edu.ph | [1]Department of Chemical Engineering, Saint Louis University, Baguio City 2600, Philippines. [2]Graduate Program, School of Engineering and Architecture, Saint Louis University, Baguio City 2600, Philippines.

Graphic abstract

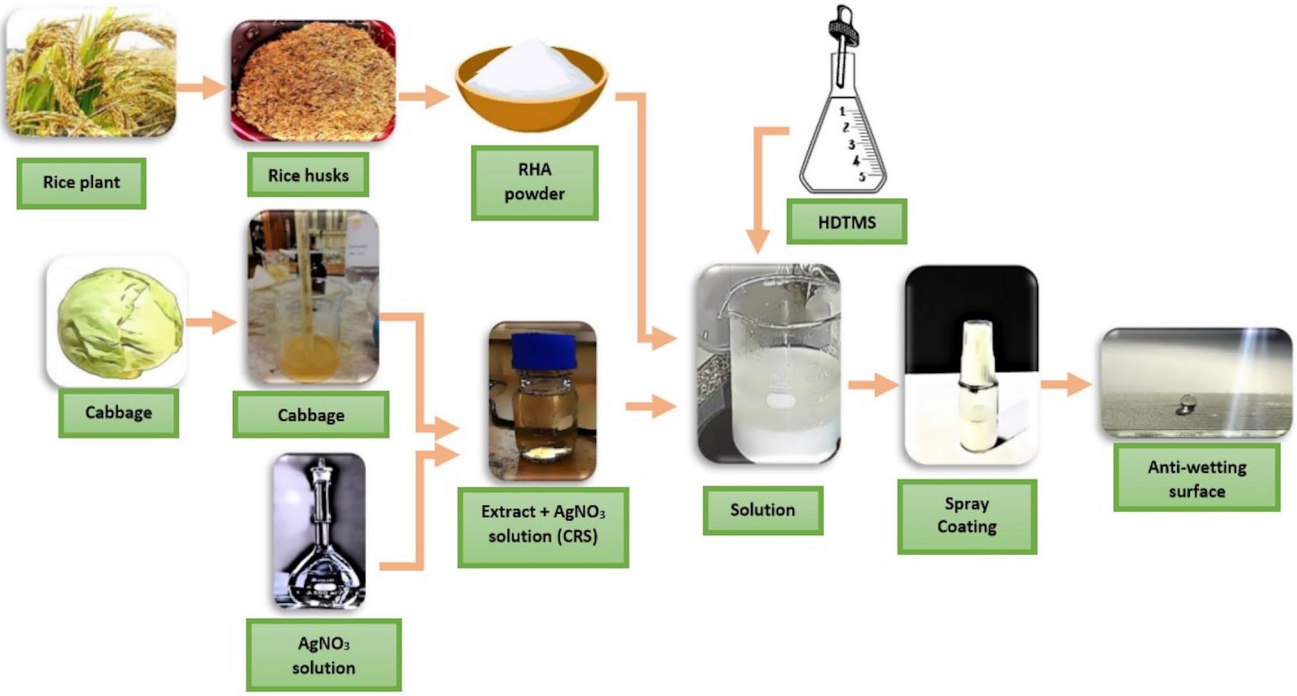

Keywords Superhydrophobicity · Coating · Silica · Silver · Self-cleaning

1 Introduction

Nature always trumps human ingenuity when it comes to the design and engineering of specialized surface that repels water instantaneously the moment it comes in touch with it [1, 2]. This is perfectly embodied by the lotus, which, upon revelation of its morphology, was biomimicked into real-life practical applications [3] such as self-cleaning, water-repellency, corrosion and chemical resistance, de-icing, and oil/water separation. Studies show that such impressive surface properties are due to a hierarchical surface structure created by convex papillose epidermal cells with a large dense sequence of three-dimensional epicuticular waxes whose forms are unequal. By peering further into this micro-nanostructure, cellular microbumps and waxy nanocrystals with low surface energy are revealed. Hence, the two basic requirements that needed to be satisfied to produce a surface of superhydrophobic nature are roughness in the micro- and nanometer scale and a coating of low surface energy [4–7].

In theory, two models of wetting behavior have been demonstrated, namely the Wenzel's and the Cassie–Baxter's. The former, also known as the petal effect, involves homogeneous wetting regime that describes a water droplet following the roughness but sticking to the surface, while the latter, also known as the lotus effect, describes the droplet that suspends above the spikes of the structure where air is trapped making the droplet roll at low sliding angles [8, 9]. The efforts made to resemble these patterns and create artificial copies have been many and diverse [2, 10, 11]. Techniques [12–14] such as plasma etching, lithography, sol-gel technology, microphase deposition, templating, chemical vapor deposition, and layer-by-layer techniques involve a rather complex method employing sophisticated equipment and instrumentation. In addition, use of fluorinated polymers, silicones, and silanes as materials of low surface energy is widespread and most artificially roughened surfaces contain a coating of these substances to make them superhydrophobic [3, 15].

One of the most promising techniques that shows great potential for wide commercial production is the nanoparticle synthesis route applied via a simple spray deposition technique. Unlike the aforementioned methods, it is a one-step process that does not require special equipment or extreme conditions (i.e. high temperature or vacuum conditions) during application. It is also relatively less expensive [6] and the nanoparticles themselves regulate

and control the nanoscale roughness of the coated surfaces. Silica particles are one of the most frequently used because of their abrasion resistance, low cost, availability, and size variety, which make them a common choice for the fabrication of superhydrophobic surfaces [6]. In addition, silica has high hardness and low refractive index elevating them further to be one of the most promising nanoparticles for the production of protective coatings [16]. However, commercially available silica particles are produced by the traditional thermal fuming method, which unfortunately results to several unwanted by-products and consumes an immense amount of energy. Hence, environmental protection, green chemistry, and energy-effective designs should be globally promoted.

Developments and applications of biomimetic and bioinspired silica using biological systems ranging from microorganisms to animals and plants through a process of biological silica formation have been reported [17, 18]. The utilization of rice (*Oryza sativa*) husk ash (RHA) as a sustainable source of silica steals the limelight not only because of its wide availability in rice-staple food countries (like many Asian countries including the Philippines) but also because it accumulates as waste of the rice milling industries [19, 20]. By following the line of reasoning henceforth presented, this study aims to formulate a coating mimicking the structure of the lotus using the spraying technique and utilizing silica from RHA instead of the fumed or pyrogenic form.

Amidst this interesting idea, however, coatings of silica suffer some stability issues such that the superhydrophobicity disintegrates to some extent with time. Based on the Derjaguin–Landau–Verwey–Overbeek (DLVO) model [21–23], nanoparticles tend to aggregate because of forces, such as interfacial attraction and van der Waals, that become significant in the micro-scale. In order to avoid agglomeration of the particles to form larger clumps and thereby decreasing the roughness, another repulsive interaction (steric and van der Waals repulsion) should be put into place by decorating the surface of the particles with other particles [24, 25]. Silver (Ag) proves to complement silica best where heterogeneous nanocomposite materials are concerned and the resultant combination exhibits biocompatibility and functionality [26].

Ag nanoparticles can be synthesized in many ways including the chemical synthesis route, the physical, and the biological [27–29]. The biological route is chosen in this study as it can be easily executed via the use of reducing agents such as plants [28, 30, 31]. Cabbage (*Brassica oleracea capitata*) is of primary interest as it is simple, environmentally-benign, and non-toxic. It is readily available and proven to have successfully reduced and capped Ag nanoparticles from $AgNO_3$ [32, 33]. From these realizations, the idea of coming up with a novel method of a more stable superhydrophobic spray coating, which is itself a bio-inspired scientific undertaking, but using sustainable and environmentally-benign methods, was conceived, and will be the watermark of this study.

2 Materials and methods

2.1 Materials

Waste rice husks were generously given by a local milling company located in the province of Pangasinan, Philippines, while cabbage was obtained and purchased from Baguio City Public Market, Philippines. 95% ethanol solution was purchased from Sigma-Aldrich, while 25% NH_4OH solution was acquired from Qualikems. Hexadecyltrimethoxysilane (HDTMS), as the bonding and adhering agent, was purchased from Hangzhou Jessica Chemical Co. Ltd., China.

2.5 N NaOH solution was prepared by dissolution of NaOH pellets (HiMedia Laboratories) in distilled water. 5 N H_2SO_4 solution was prepared by diluting concentrated H_2SO_4 (98%, RCI Labscab Ltd.) while 6 N HCl by dilution of 37% HCl solution (Macron Fine Chemicals). $AgNO_3$ (99.98%, granules, BDH Laboratory) was used to prepare 1 mM $AgNO_3$ solution by dissolution in deionized distilled water. All other chemicals were used as received.

2.2 Synthesis of silica-containing RHA from rice husks

Rice husks were initially cleaned by washing with distilled water and putting into an oven for complete evaporation of moisture. The dried rice husks were then fired in a muffle furnace at 700 °C for 6 h to obtain the ash form. To extract silica, 10 g of the latter, after subsequent cooling, was mixed with 80 mL of 2.5 N NaOH, solubilizing the silica present into sodium silicate. The resulting mixture was refluxed for 3 h to increase the silicate solubility. Afterwards, the solution was filtered to remove any impurities while simultaneously adding boiling water into it. After allowing the filtrate to cool, 5 N H_2SO_4 was slowly added until acidic and precipitate begins to form. The solution was then made slightly basic by the addition of concentrated NH_4OH and heated to dryness. Subsequent purification steps involved refluxing the dried precipitate with 6 N HCl for 4 h, washing the precipitate repeatedly with deionized water to render it acid-free, dissolving the precipitate again with 2.5 N NaOH with continuous stirring for 10 h, and finally adding H_2SO_4 to obtain back the RHA precipitate. This was then followed by filtration of the mixture and drying of the silica-containing RHA (or simply RHA) residue at 50 °C for 48 h [19, 34, 35].

2.3 Synthesis of cabbaged-reduced Ag (CRS) particles

The cabbage leaves were washed thoroughly with deionized distilled water and air-dried. The leaves were then cut into about 10-mm size strips and boiled in distilled water for 15 min. The extract from the cabbage was filtered, transferred to a bottle covered with aluminum foil, and refrigerated until use.

10 mL of the cabbage extract was added to 90 mL of 1 mM $AgNO_3$ solution contained in a bottle covered with aluminum foil to avoid exposure to light. The resulting solution was shaken and incubated for 15 min at 27 °C, after which, the solution's color changed from pale yellow to honey brown, thus, indicating the formation of Ag particles. The solution was further set aside for 24 h to ensure maximum reduction of Ag^+ to metal Ag [32, 33].

2.4 Preparation of the spray formulations

7 mL of HDTMS was added drop wise to 95% ethanol solution with vigorous stirring for 15 min at room temperature, after which, stirring was continued for 3 h more. RHA was then added in increasing amounts (10, 12.5, 15, 17.5, 20, 22.5, and 25 wt%) to the prepared silane-alcohol solution and the different formulation coatings were stirred for 3 h to attain maximum RHA dispersion. Using the most superhydrophobic coating, the RHA/CRS solution was finally prepared in a 10:1 volume ratio. A commercially available, hand-powered plastic spray bottle was used to contain and apply the coatings from a distance of 2–3 in. to the different surfaces (i.e., glass, masking tape, and paper). After drying for 5 min at room temperature, the coating thickness was estimated at around 50 µm.

2.5 Instrumentation

Static water CA was determined by placing approximately 5 µL of water droplets on the surface of the substrates and measured by an Image-J computer software. Fourier-transform infrared (FT-IR) spectroscopy was done using a Shimadzu IRPrestige 21 FTIR spectrometer, which scanned between 4000 and 400 cm^{-1} with a resolution of 2 cm^{-1} (128 scans were performed and averaged). Thermogravimetric analysis (TGA) was made possible using a Perkin Elmer TGA 4000 under a continuous nitrogen purge (20.0 mL/min). The weight loss was monitored as around 10 mg weight of the sample was heated at a rate of 10 °C/min to a maximum temperature of 800 °C.

To detect the presence of Ag, atomic absorption spectroscopy (AAS) via a 55 AA Atomic Absorption Spectrometer and ultraviolet-visible (UV-VIS) spectroscopy using a Perkin Elmer Lambda 25 Spectrometer were performed. For the morphology and elemental composition, scanning electron microscopy (SEM) was performed via a JEOL JSM 6010LV (using an iridium coating) coupled with OXFORD XMax80 Energy-Dispersive X-Ray (RDX) spectrometer for the energy dispersive X-ray (EDX) analysis.

3 Results and discussion

3.1 Characterizations

FT-IR was done to confirm the presence of silica in the RHA. Based on the spectrum shown in Fig. S1, the following bands were observed: the broad band from 3700 to 3200 cm^{-1} is a combination band due to the stretching vibrations of Si–OH and H–OH; the bands stretching from 2250 to 2100 cm^{-1} are due to the Si–H stretching; the band near 1630 cm^{-1} corresponds to the bending vibrations of H–OH; 1115 (the strongest band that signatures the presence of silica) and the band near 800 cm^{-1} are attributed to the asymmetric and symmetric stretching of Si–O–Si, respectively [36].

The presence of silica in RHA was further clarified via element analysis using EDX spectroscopy. RHA-coated and uncoated masking tapes were used as the samples in this experiment and the corresponding spectra are shown in Fig. 1. The spectrum in Fig. 1a showed elemental peaks, which are consistent with the composition of a typical masking tape [37]. Figure 1b, on the other hand, displayed an additional peak for Si and an increase in the peak intensity for O, which confirm the presence of silica in the RHA. It has to be noted that the other peaks correspond to the composition of the uncoated masking tape, which are still evident due to the high keV energy of the beam used such that it is able to penetrate through the substrate.

The identity of silica-containing RHA in terms of thermal stability was also analyzed and the resulting thermogram is shown in Fig. S2. It is obvious that no significant amount of the RHA decomposes as represented by the curve running almost parallel to the x-axis, experiencing only 1.74% decrease in weight at 100 °C (due to loss of moisture content) and approximately 3.0% at 800 °C. It therefore further proves that the RHA is composed mainly of SiO_2 and many literatures report its excellent thermal stability even at high temperatures [38].

EDX results were also collected for the RHA/CRS coated surface, unfortunately, Ag was not detected since added amount was very minimal, thus, a need to perform UV-VIS and AAS to detect the presence of CRS. The corresponding UV-VIS spectra for RHA and RHA/CRS are shown in Fig. S3 and it can be seen that the two project similar curve patterns, with the RHA/CRS spectrum displaying a lower absorbance than that of the RHA near 300 nm. The

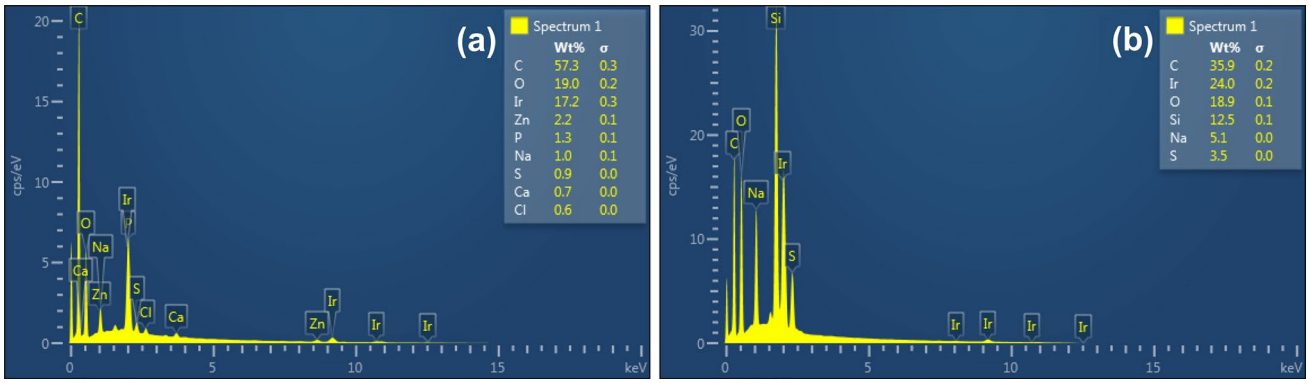

Fig. 1 EDX spectra of **a** uncoated and **b** RHA-coated masking tape

decrease in absorbance can be attributed to the stabilizing effect and capping properties of the Ag particles [39], which prevented some possible RHA particle agglomeration. Accumulation of particles results in greater absorbance (as the case for RHA) while the opposite results in lower absorbance [40, 41], both of which are seen near 300 nm. AAS experiment, on the other hand, for the CRS solution yielded a Ag concentration of 111 ppm. This was also verified qualitatively by the appearance of a dark brownish-honey color of the CRS solution (Fig. S4), which is due to the Ag's property of bending light known as surface plasmon resonance [42, 43]. Hence, this confirms the presence of Ag in the CRS solution and validates its stabilizing and capping effects as observed by the UV-VIS.

3.2 Wetting behavior and stability

Figure S5 shows the contact angle bar graphs made with the different surfaces at different RHA loadings. It is apparent that in all the surfaces, the coating with the 10 wt% RHA was not able to acquire a reasonable CA (i.e. 130°–145°) to make it superhydrophobic. With an added RHA (i.e. coating with 12.5 wt%), the coated surfaces were able to reach the superhydrophobicity level as evidenced by the CA values of greater than 150°. This is an indication that the RHA particles were able to impart sufficient roughness which, based on the Wenzel [8] or the Cassie–Baxter [9] model, introduces extreme anti-wetting behavior. In addition, the bar graphs showed a decrease in the CA values with increasing RHA content (15 to 25 wt%). This implies that excess addition of the RHA results in particle aggregation that downgrades the mechanical integrity of the coating itself and eventually reducing the roughness. Hence, the 12.5 wt% is taken as the best RHA loading, which is used (and named herein as RHA/CRS), for the purpose of simplification for the rest of the discussion. It is also evident that this RHA coating achieved superhydrophobicity without the presence of a low surface energy material. Such an achievement can be explained by the presence of carbonaceous components and functional groups (as evidenced by a high C peak in the EDX spectrum and IR peaks near 1750 cm^{-1}, 3000 cm^{-1}, and 2300–2000 cm^{-1}) on the RHA surface that may have developed during the firing of the rice husks. Such presence of carbonaceous components can significantly lower the surface energy of any given material. Moreover, the incorporation of CRS to the 12.5% RHA contributed to the superhydrophobicity of the coated surfaces to a certain degree as evidenced by a slight increase in the CA values shown in Fig. 2. This shows that adding intermittent new particles between the deposited RHA particles further increases the roughness, hence the superhydrophobicity.

Shang et al. [44] prepared silica-based superhydrophobic films on glass substrates, in which the silica particles were synthesized via the sol-gel process using tetraethylorthosilicate (TEOS) as the main starting material and

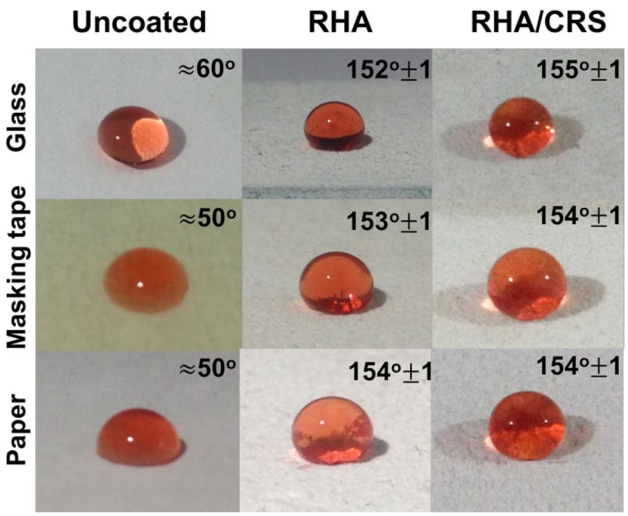

Fig. 2 Static water CA of uncoated, RHA-coated, and RHA/CRS-coated glass, masking tape and paper substrates

trideca-fluoro-1,1,2,2-tetrahydrooctyldimethylchlorosilane (TFCS) as the silane surface modifying agent. The CA of the pristine silica coating was found to be 115°. Upon surface modification with TFCS, the resulting coating showed a superhydrophobic behavior with a CA of 150°. Another study by Daoud et al. [45] made use of TEOS, HDTMS, and 3-glycidoxypropyltrimethoxysilane (GPTMS) to synthesize silica sol via cohydrolysis and polycondensation methods. Results show that the silica film coating yielded a CA of 141°, which is barely superhydrophobic. It is apparent that these studies describe the synthesis of silica particles via the commonly known sol-gel route utilizing TEOS as the main source of SiO_2. In our study, we present a less complex process of obtaining SiO_2 from rice husks and modification with Ag particles to prevent the agglomeration and aid in further stabilization of SiO_2 particles. The utilization of rice husks as the main source of SiO_2 and cabbage, a vegetable, as a reducing agent in the synthesis of Ag particles makes our preparation method easier and eco-friendlier as these materials are non-toxic and can be readily acquired. In addition, our pristine silica coatings yielded higher CA values (up to 154°) than those obtained from the aforementioned studies. With the inclusion of Ag particles, even higher CA values were achieved.

Figure 3 contrasts the anti-wettability of the RHA/CRS coated on paper with that of the uncoated one. It can be observed that the RHA/CRS exhibits the Cassie–Baxter state [9] (or the lotus effect) where water droplets sit atop the rough surface, which contain many micro- and nanodepressions of trapped air that minimizes the contact area. As a consequence, droplets of water easily roll off the surface at a sliding angle of ~5° and can remove any dirt present on the surface. Therefore, the coating is said to display self-cleaning property. The complete video clips for this experiment can be viewed by watching V1 and V2 in the Supplementary Information. V3 is also a useful video clip that demonstrates the lotus effect where a water droplet does not adhere to the coating.

Figure S6 provides an additional argument to favor the coating with RHA/CRS against that of RHA only. The CA was measured every 30 s for a total period of 10 min for a steady water droplet (i.e. allowing the droplet to stay still on the surface) to investigate how long the two different coated surfaces can hold and maintain a droplet in its spherical form until spreading. It can be observed that upon extended contact time, the water droplet rapidly spread on the RHA surface as evidenced by a fast decreasing CA (with a final CA of ~77° from an initial of ~153° in a span of 10 min). This means that the RHA coating is not resistant enough for a prolonged water droplet contact.

On the other hand, the coating with the CRS showed an improved water resistance and its difference from the RHA coating is easily discernible. Over the 10-min span of time, the shape of the water droplet did not seem to change much as evidenced by a very sluggish but gradual drop in CA. It was observed that after 10 min, the CA dropped from ~155° to a final of only ~140°, after which it remained almost constant thereafter. This shows that the placement of the CRS between the deposited RHA particles, not only improves roughness and thereby the CA, but also provides repulsive forces between the RHA particles, hindering agglomeration in time, thus maintaining the anti-wetting behavior for an extended period of time. Application-wise,

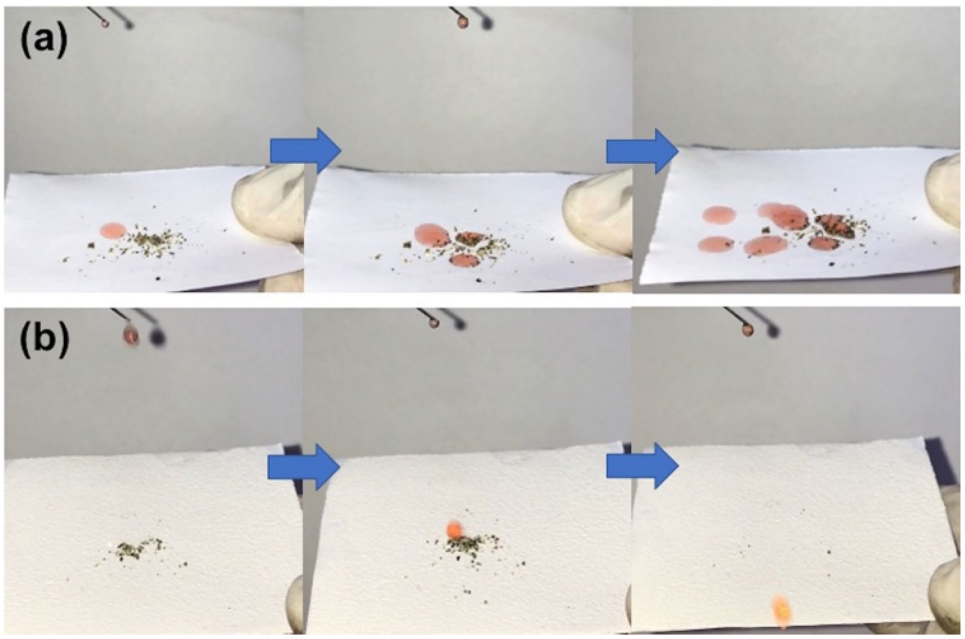

Fig. 3 Screenshots of water droplets as they fall on top of the **a** uncoated and **b** RHA/CRS-coated paper substrate demonstrating self-cleaning effect

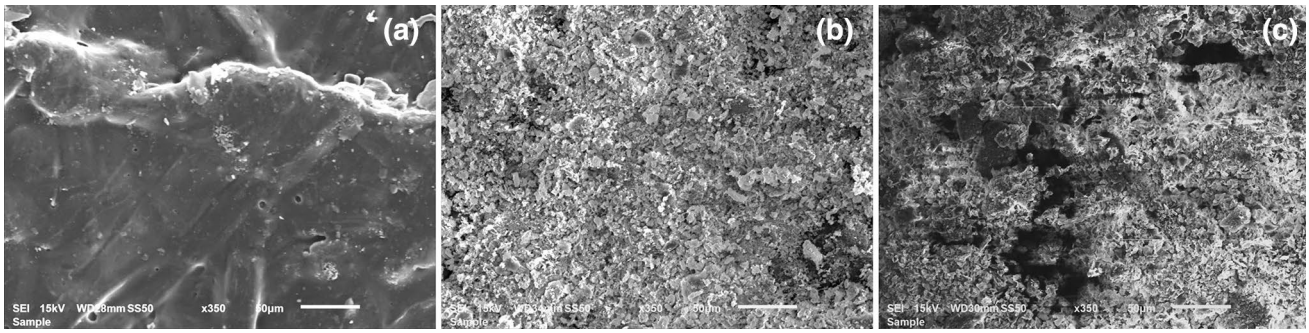

Fig. 4 SEM images of the **a** uncoated, **b** RHA-coated, and **c** RHA/CRS-coated masking tape with 50 µm scale bar

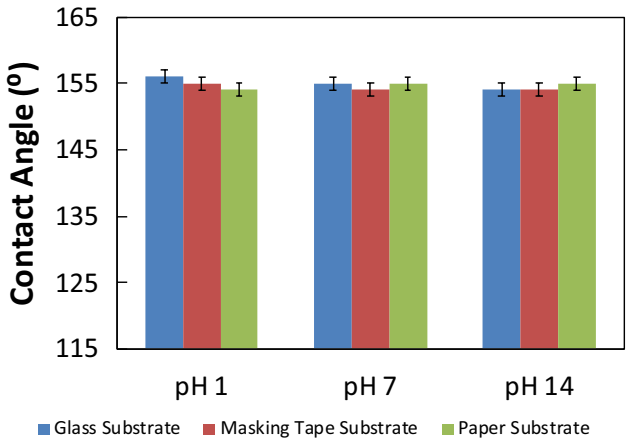

Fig. 5 Static water CA of RHA/CRS at pH values of 1, 7, and 14

the RHA/CRS coating is excellent for protection of surfaces against water splashes.

3.3 Surface morphology

Figure 4 displays the SEM images of the uncoated masking tape with the corresponding RHA- and RHA/CRS-coated ones. It is apparent that the surface of the uncoated substrate does not possess a rough structure as would be expected from a masking tape. With the RHA coated on it, the resulting morphology revealed roughness with micro- and possibly nano-hierarchical structure, which is the prime reason why the surface exhibits anti-wetting behavior as evidenced by the measured CA. Similarly, densely-packed particles with many small depressions and hierarchical features, which impart roughness, are spotted for the RHA/CRS-coated surface.

3.4 Resistance to pH, mechanical integrity, and durability

Figure 5 shows the comparison of CA of neutral water for the different RHA/CRS-coated substrates with those of extremely acidic and basic conditions. It is interesting to note that the coated surfaces remarkably displayed superhydrophobicity (where CA ranging from 154° to 156° with ±1 difference) as well for water with pH values of 1 and 14. In addition, it was observed that the water droplets for these conditions easily rolled off when the surfaces were disturbed or tilted at a minimum angle of ~5°. Thus, it can be suggested that such coated surfaces are suitable for use under harsh conditions.

Table 1 Static water CA values showing the mechanical integrity and durability of the RHA/CRS coating

	Application of force from thumb		Span of 4 weeks	
	Before	After	Before	After
Glass	155°±1°	155°±1°	151°±1°	155°±1°
Masking tape	154°±1°	155°±1°	152°±1°	155°±1°
Paper	154°±1°	154°±1°	153°±1°	154°±1°

Table 1 presents the CA values before and after the application of force from a thumb. It can be noticed that the application of a force did not in a way negatively affect the coated surfaces with the CA values unchanged. This proves that even if the coated surfaces experience touches here and there and contact with other materials, the coating will still be able to maintain the desirable anti-wetting property that it provides.

We also measured the CA at two different points in time spanning a 4-week period (Table 1). It can be observed that the measured CA values have not only been maintained but improved even more. When decorated with CRS, the RHA particles are being hindered from agglomerating with each other due to induced repulsive forces (i.e. van der Waals), electrostatic forces, and steric/confining or jamming forces, which are caused by the confining micro- and nanoparticle that may either be linear or exponential [46]. Additionally, this durability can be attributed to further separation of water from the coating as time passed by leaving a more defined structure.

4 Conclusion

It is therefore concluded that the silica-containing RHA can be used as an ingredient, with the aid of HDTMS, in a spray coating to attain superhydrophobicity. Conversely, CRS in minimal concentrations, can be added to impart surface structure stability. Based on the CA measurements, 12.5 wt% RHA was determined to be the best loading as it gives the best anti-wetting property due to the roughness being imparted as evidenced by SEM. In addition, the inclusion of CRS does not only slightly improve the superhydrophobicity, but proves to be a potent solution to stability issues for any silica-containing coating as it prevents self-agglomeration of the RHA particles upon continued contact with water. Furthermore, the RHA/CRS coating possesses self-cleaning property in which the water droplets roll off the surface easily, force thumb resistance in which the anti-wetting behavior is unaffected by any touches, high thermal stability, and durability. Our method of preparation for these superhydrophobic coatings is fairly simple as it does not involve complicated steps found in the traditional sol-gel process. It is also an environment-friendly process as the materials used (i.e. rice husks as the source of SiO_2 and cabbage as a reducing agent in the synthesis of Ag) are easily available and non-toxic. As an added-value, our coatings did not need a low surface energy component such as a polymer matrix or a fluorinated material to achieve superhydrophobicity as they already exhibited low surface energy due to the presence of carbonaceous functional groups that may have evolved during the silica preparation from rice husks. Moreover, the blending or decorating of nanoparticles with another set of particles (in our case, decorating the SiO_2 particles with Ag particles) is considered a new way of enhancing the anti-wettability and roughness structure stability of superhydrophobic coatings without having the need to incorporate a low surface energy polymer matrix. It is thought that the RHA/CRS coating has potential for industrial large scale production and deserves additional researches for further development.

Compliance with ethical standards

Conflict of interest On behalf of all authors, the corresponding author states that there is no conflict of interest.

References

1. Latthe SS, Gurav AB, Maruti CS, Vhatkar RS (2012) Recent progress in preparation of superhydrophobic surfaces: a review. J Surf Eng Mater Adv Technol 2:76
2. Yao X, Song Y, Jiang L (2011) Applications of bio-inspired special wettable surfaces. Adv Mater 23:719–734
3. Simpson JT, Hunter SR, Aytug T (2015) Superhydrophobic materials and coatings: a review. Rep Prog Phys 78:086501
4. Wang J, Chen H, Sui T, Li A, Chen D (2009) Investigation on hydrophobicity of lotus leaf: experiment and theory. Plant Sci 176:687–695
5. Yu Y, Zhao Z-H, Zheng Q-S (2007) Mechanical and superhydrophobic stabilities of two-scale surfacial structure of lotus leaves. Langmuir 23:8212–8216
6. Cohen N, Dotan A, Dodiuk H, Kenig S (2016) Superhydrophobic coatings and their durability. Mater Manuf Process 31:1143–1155
7. Meng L-Y, Park S-J (2014) Superhydrophobic carbon-based materials: a review of synthesis, structure, and applications. Carbon Lett 15:89–104
8. Wenzel RN (1936) Resistance of solid surfaces to wetting by water. Ind Eng Chem 28:988–994
9. Cassie A, Baxter S (1944) Wettability of porous surfaces. Trans Faraday Soc 40:546–551
10. Jeevahan J, Chandrasekaran M, Joseph GB, Durairaj R, Mageshwaran G (2018) Superhydrophobic surfaces: a review on fundamentals, applications, and challenges. J Coat Technol Res 15:231–250
11. Caldona EB, Albayalde JMC, Aglosolos AMP, Bautista KS, Tavora MD, Cabalza SAP, Diaz JRO, Mulato MD (2019) Titania-containing recycled polypropylene surfaces with photo-induced reversible switching wettability. J Polym Environ 27:1564–1571
12. Dimitrakellis P, Gogolides E (2018) Hydrophobic and superhydrophobic surfaces fabricated using atmospheric pressure cold plasma technology: a review. Adv Colloid Interface Sci 254:1–21
13. Jiaqiang E, Jin Y, Deng Y, Zuo W, Zhao X, Han D, Peng Q, Zhang Z (2018) Wetting models and working mechanisms of typical surfaces existing in nature and their application on superhydrophobic surfaces: a review. Adv Mater Interfaces 5:1701052–1701091
14. Nguyen-Tri P, Tran HN, Plamondon CO, Tuduri L, Vo D-VN, Nanda S, Mishra A, Chao H-P, Bajpai A (2019) Recent progress in the preparation, properties and applications of superhydrophobic nano-based coatings and surfaces: a review. Prog Org Coat 132:235–256
15. Ma Y, Cao C, Hou C (2018) Preparation of super-hydrophobic cotton fabric with crosslinkable fluoropolymer. In: Applied sciences in graphic communication and packaging. Springer, pp 955–962
16. Caldona EB, De Leon ACC, Thomas PG, Naylor DF III, Pajarito BB, Advincula RC (2017) Superhydrophobic rubber-modified polybenzoxazine/SiO2 nanocomposite coating with anticorrosion, anti-ice, and superoleophilicity properties. Ind Eng Chem Res 56:1485–1497
17. Davidson S, Lamprou DA, Urquhart AJ, Grant MH, Patwardhan SV (2016) Bioinspired silica offers a novel, green, and biocompatible alternative to traditional drug delivery systems. ACS Biomater Sci Eng 2:1493–1503
18. Zan G, Wu Q (2016) Biomimetic and bioinspired synthesis of nanomaterials/nanostructures. Adv Mater 28:2099–2147
19. Haq IU, Akhtar K, Malik A (2014) Effect of experimental variables on the extraction of silica from the rice husk ash. J Chem Soc Pak 36:382
20. Pode R (2016) Potential applications of rice husk ash waste from rice husk biomass power plant. Renew Sustain Energy Rev 53:1468–1485
21. Derjaguin B (1941) Theory of the stability of strongly charged lyophobic sols and the adhesion of strongly charged particles in solutions of electrolytes. Acta Physicochim USSR 14:633–662

22. Deryaguin B, Landau L (1945) Theory of the stability of strongly charged lyophobic sols and the coalescence of strongly charged particles in electrolytic solutions. Sov Phys JETP 15:633
23. Verwey EJW, Overbeek JTG, Overbeek JTG (1999) Theory of the stability of lyophobic colloids. Courier Corporation, New York
24. Pacakova B, Mantlikova A, Niznansky D, Kubickova S, Vejpravova J (2016) Understanding particle size and distance driven competition of interparticle interactions and effective single-particle anisotropy. J Phys: Condens Matter 28:206004
25. Frandsen C, Mørup S (2003) Inter-particle interactions in composites of antiferromagnetic nanoparticles. J Magn Magn Mater 266:36–48
26. Santagata A, Guarnaccio A, Pietrangeli D, Szegedi Á, Valyon J, De Stefanis A, De Bonis A, Teghil R, Sansone M, Mollica D (2015) Production of silver-silica core-shell nanocomposites using ultra-short pulsed laser ablation in nanoporous aqueous silica colloidal solutions. J Phys Appl Phys 48:205304
27. Rauwel P, Rauwel E, Ferdov S, Singh MP (2015) Silver nanoparticles: synthesis, properties, and applications. Adv Mater Sci Eng 2015:1–2
28. Tran QH, Le A-T (2013) Silver nanoparticles: synthesis, properties, toxicology, applications and perspectives. Adv Nat Sci Nanosci Nanotechnol 4:033001
29. Iravani S, Korbekandi H, Mirmohammadi S, Zolfaghari B (2014) Synthesis of silver nanoparticles: chemical, physical and biological methods. Res Pharm Sci 9:385
30. Kalaiselvi M, Subbaiya R, Selvam M (2013) Synthesis and characterization of silver nanoparticles from leaf extract of *Parthenium hysterophorus* and its anti-bacterial and antioxidant activity. Int J Curr Microbiol Appl Sci 2:220–227
31. Anandalakshmi K, Venugobal J, Ramasamy V (2016) Characterization of silver nanoparticles by green synthesis method using *Pedalium murex* leaf extract and their antibacterial activity. Appl Nanosci 6:399–408
32. Deb S (2014) Synthesis and characterisation of silver nanoparticles using *Brassica oleracea capitata* (Cabbage) and *Phaseolus vulgaris* (French Beans): a study on their antimicrobial activity and dye degrading ability. Int J ChemTech Res 6:3909–3917
33. Tamileswari R, Nisha M, Jesurani S (2015) Green synthesis of silver nanoparticles using *Brassica oleracea* (cauliflower) and *Brassica oleracea capitata* (cabbage) and the analysis of antimicrobial activity. Int J Eng Res Technol 4:1071–1074
34. Thuadaij N, Nuntiya A (2008) Synthesis and characterization of nanosilica from rice husk ash prepared by precipitation method. J Nat Sci Spec Issue Nanotechnol 7:59–65
35. de Lima SPB, de Vasconcelos RP, Paiva OA, Cordeiro GC, de Chaves MRM, Toledo Filho RD, de Fairbairn EMR (2011) Production of silica gel from residual rice husk ash. Quím Nova 34:71–75
36. Fidalgo A, Ilharco LM (2001) The defect structure of sol–gel-derived silica/polytetrahydrofuran hybrid films by FTIR. J Non-Cryst Solids 283:144–154
37. Merrill R, Bartick E (2000) Analysis of pressure sensitive adhesive tape: I. Evaluation of infrared ATR accessory advances. J Forensic Sci 45:93–98
38. Joo SH, Park JY, Tsung C-K, Yamada Y, Yang P, Somorjai GA (2009) Thermally stable Pt/mesoporous silica core–shell nanocatalysts for high-temperature reactions. Nat Mater 8:126
39. Wei L, Lu J, Xu H, Patel A, Chen Z-S, Chen G (2015) Silver nanoparticles: synthesis, properties, and therapeutic applications. Drug Discov Today 20:595–601
40. Jeon H-J, Yi S-C, Oh S-G (2003) Preparation and antibacterial effects of Ag–SiO2 thin films by sol–gel method. Biomaterials 24:4921–4928
41. Flores J, Torres V, Popa M, Crespo D, Calderón-Moreno J (2008) Preparation of core–shell nanospheres of silica–silver: SiO2@ Ag. J Non-Cryst Solids 354:5435–5439
42. Thomas S, Nair SK, Jamal EMA, Al-Harthi S, Varma MR, Anantharaman M (2008) Size-dependent surface plasmon resonance in silver silica nanocomposites. Nanotechnology 19:075710
43. Mock J, Barbic M, Smith D, Schultz D, Schultz S (2002) Shape effects in plasmon resonance of individual colloidal silver nanoparticles. J Chem Phys 116:6755–6759
44. Shang H, Wang Y, Limmer S, Chou T, Takahashi K, Cao G (2005) Optically transparent superhydrophobic silica-based films. Thin Solid Films 472:37–43
45. Daoud WA, Xin JH, Tao X (2004) Superhydrophobic silica nanocomposite coating by a low-temperature process. J Am Ceram Soc 87:1782–1784
46. Min Y, Akbulut M, Kristiansen K, Golan Y, Israelachvili J (2008) The role of interparticle and external forces in nanoparticle assembly. Nat Mater 7:527